Time resolved rutile U/Pb data derived from LA-ICPMS – a case study from the North Pamir

Johannes Rembe[1], Renjie Zhou[2], Edward R. Sobel[1], Jonas Kley[3], and Rasmus Thiede[4]

[1]University of Potsdam, Earth and Environmental Sciences, Geology, Potsdam, Germany (jrembe@uni-potsdam.de), [2]The University of Queensland, School of Earth and Environmental Sciences, Brisbane, Australia, [3]Georg-August-Universität Göttingen, Geoscience Center, Göttingen, Germany, [4]Christian-Albrechts-Universität Kiel, Institute for Geosciences, Kiel, Germany

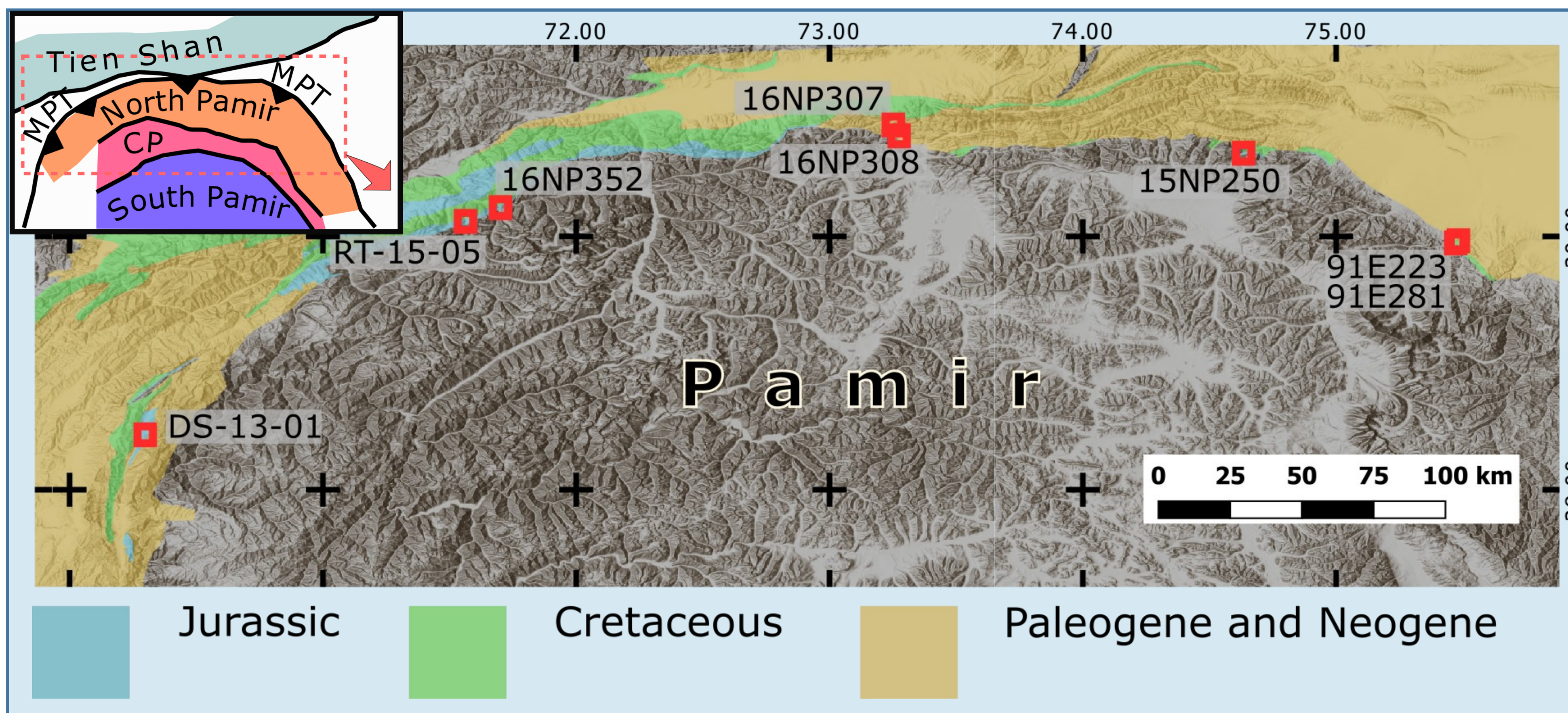

Figure 1 : Map of the distribution of Jurassic to Neogene strata in the Pamir foreland. Samples were taken in the External Pamir, the footwall of the Main Pamir thrust (MPT). The inset map shows regional tectonic domains (CP: Central Pamir).

1. Introduction

The External Pamir reveals a continuous sedimentary record from Jurassic to Neogene time (fig. 1). We use detrital rutile data to characterize their source areas.

Rutile is a common accessory mineral in all types of rocks. Metamorphic rutile may grow under greenschist to eclogite facies conditions and could be found in meta-mafic rocks which typically contain few zircon. In provenance analysis, detrital rutile may supplement detrital zircon for that they may reveal additional thermal or metamorphic information regarding sediment source.

Rutile could be challenging to analyse with U-Pb geochronology because of their varying amounts of common lead and low U (typically between 3 and 130 ppm) (Mezger et al., 1989). Due to the presence of common lead, a common lead correction is necessary for calculating rutile U-Pb ages. Following an approach presented by Stockli et al. (2017), we subdivided the signal of each laser ablation spot into 10 to 12 time-slices that resulted in an age-depth profile (Odlum & Stockli, 2020). We compare our time-sliced ages with ages corrected by the Stacey-Kramers approach (Stacey & Kramers, 1975).

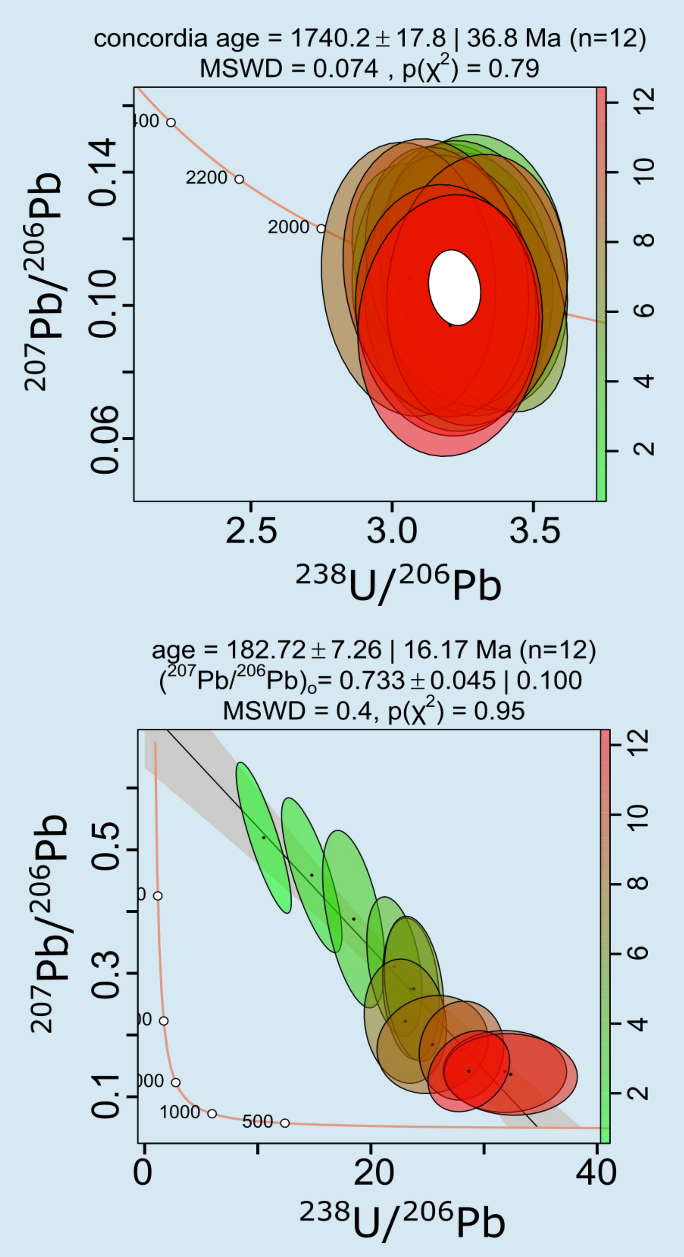

Figure 2 : Example single-grain time-slice data. (a) A concordant grain and (b) a discordant grain (both from 16NP308). Colour coding from green to red is based on the depth of ablation where green represents the first slice. A lower intercept age is calculated for discordant grain (see Figure 3).

Figure 3: Flow chart for age calculation with R codes.

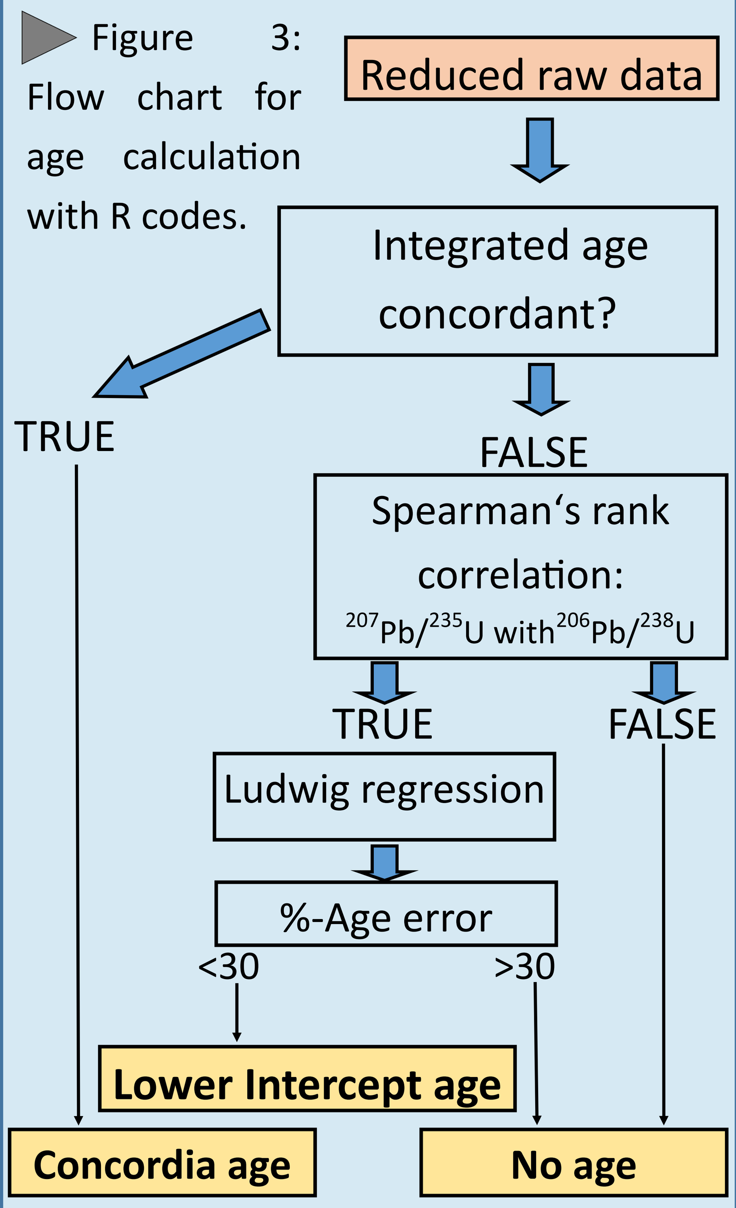

2. Motivation

Collision of the South-, Central- and North Pamir terranes caused the Late Triassic to Early Jurassic Cimmerian orogeny (Villarreal et al., 2019; Schwab et al., 2004). This major tectonic event was connected with obduction of metamorphic nappes. We aim to identify a Cimmerian age peak in detrital rutile data to constrain the onset of North– and Central Pamir sedimentation into the External Pamir sedimentary basin. Furthermore we test an internal common lead correction approach for the first time on detrital rutile grains.

3. Method

We used a laser ablation inductively coupled plasma (LA-ICPMS) system for data acquisition during two measurement sessions. Rutile grains were mounted and polished to expose internal surface. Laser ablation was conducted with 50-µm round spots and 15-20 s ablation time. Rutile DXK (Shi et al., 2012) and R632 (Axelsson et al., 2018) were used as primary reference materials. Data reduction was done in Iolite (Paton et al., 2011). Time integrated and ~1 s time-sliced data were obtained for each ablation spot.

Time-sliced data of discordant grains may yield lower intercept ages, such as observed in rapidly cooled apatite (Odlum & Stockli, 2020). The time-slices reveal depth profiles of the rutile grain, which have three patterns: (1) dense cluster of concordant time-slices, (2) dense cluster of discordant time-slices and (3) time-slices along a discordia in Tera-Wasserburg diagram (fig. 2).

4. Results and Conclusion

The use of time-slicing and internal correction for common lead provides information about intra-grain spatial distribution of Isotope ratios. Age results largely agree with Stacey-Kramers corrected values. However, there are differences in age peaks (fig. 4). We show that Eo-Cimmerian ages could be found in strata younger than the lower Jurassic. In the lower Neogene strata, youngest rutile ages are 37 to 40 Ma with the youngest major age peak located at the Cimmerian (~211 Ma). Detrital rutile ages in the External Pamir reveal Precambrian (1700 - 2100 Ma) and early Palaeozoic (400 - 500 Ma) source rocks. Late Triassic, Cimmerian (200 - 220Ma), ages are only observed in the late Neogene sample 16NP307.

Figure 4 : Kernel density estimate (KDE) plots and histogram of rutile ages from Jurassic to Neogene sandstone strata of the external Pamir. The left column provides sample name, age of the sampling unit, the youngest rutile (*rt) age, and the youngest concordant zircon age (*zr). For each sample, internally corrected and Stacey-Kramers corrected ages are plotted. Age peaks were calculated with the peakfit function in IsoplotR (Vermeesch, 2018).

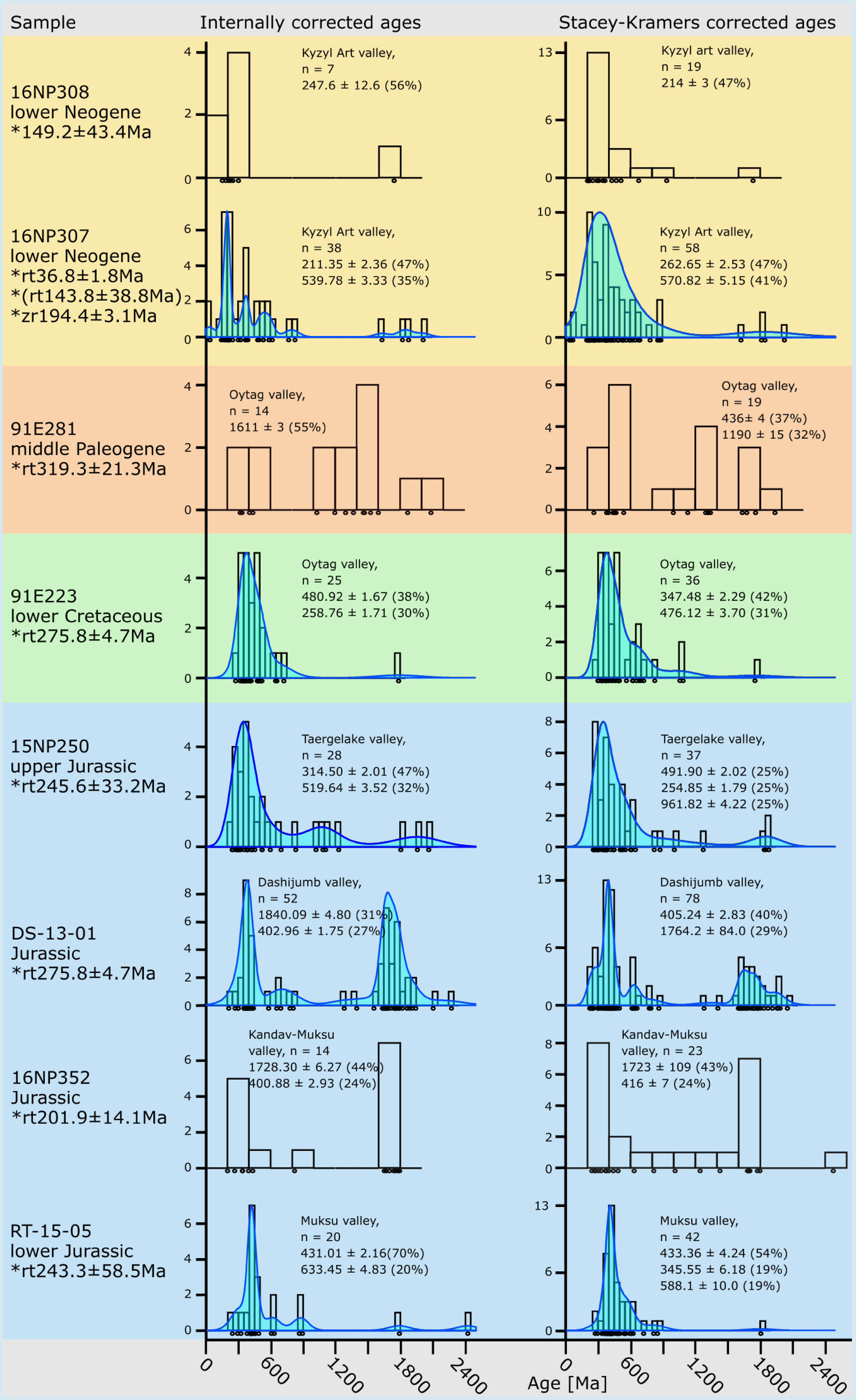

References Axelsson, E., Pape, J., Berndt, J., Corfu, F., Mezger, K., Raith, M.M., 2018. Rutile R632–A new natural reference material for U-Pb and Zr determination. Geostandards and Geoanalytical Research 42 (3), 319–338.; Mezger, K., Hanson, G.N., Bohlen, S.R., 1989. High-precision UPb ages of metamorphic rutile: application to the cooling history of high-grade terranes. Earth and Planetary Science Letters 96 (1-2),; Odlum, M.L., Stockli, D.F., 2020. Geochronologic constraints on deformation and metasomatism along an exhumed mylonitic shear zone using apatite U-Pb, geochemistry, and microtextural analysis. Earth and Planetary Science Letters 538; Paton, C., Hellstrom, J., Paul, B., Woodhead, J., Hergt, J., 2011. Iolite: Freeware for the visualisation and processing of mass spectrometric data. Journal of Analytical Atomic Spectrometry 26 (12), 2508–2518.; Schwab, M., Ratschbacher, L., Siebel, W., McWilliams, M., Minaev, V., Lutkov, V., Chen, F., Stanek, K., Nelson, B., Frisch, W., Wooden, J.L., 2004. Assembly of the Pamirs: Age and origin of magmatic belts from the southern Tien Shan to the southern Pamirs and their relation to Tibet. Tectonics 23 (4); Shi, G., Li, X., Li, Q., Chen, Z., Deng, J., Liu, Y., Kang, Z., Pang, E., Xu, Y., Jia, X., 2012. Ion microprobe U-Pb age and Zr-in-rutile thermometry of rutiles from the Daixian rutile deposit in the Hengshan Mountains, Shanxi Province, China. Economic Geology 107 (3), 525–535.; Stacey, J.S., Kramers, J.D., 1975. Approximation of terrestrial lead isotope evolution by a two-stage model. Earth and Planetary Science Letters 26 (2), 207–221.; Stockli, D.F., Boyd, P., Galster, F., 2017. Intra-grain common Pb correction in apatite by LA-ICP-MS depth profiling and implications for detrital apatite U-Pb dating. EGU General Assembly Abstract Volume.; Vermeesch, P., 2018. IsoplotR: a free and open toolbox for geochronology. Geoscience Frontiers 9 (5), 1479–1493.; Villarreal, D.P., Robinson, A.C., Carrapa, B., Worthington, J., Chapman, J.B., Oimahmadov, I., Gadoev, M., MacDonald, B., 2019. Evidence for Late Triassic crustal suturing of the Central and Southern Pamir. Journal of Asian Earth Sciences: X.